JOURNAL OF MATERIALS SCIENCE 16 (1981) 477–482

Particle impact damage in silicon nitride at 1400° C

D. A. SHOCKEY, D. C. ERLICH, K. C. DAO*
Poulter Laboratory, SRI International, Menlo Park, CA 94025, USA

Impacts of tungsten carbide spheres on Si_3N_4 produced elastic fracture behaviour (ring and cone cracks) at room temperature, but elastic–plastic fracture behaviour (plastic impressions and radial cracks) at 1400° C. In contrast, no change in fracture pattern at the two temperatures was produced by impact with steel spheres. These results may be explained by the relative abilities of the impacting spheres to cause plastic flow at the impact site and hence to alter the stress distribution in the Si_3N_4 specimens. The type and extent of damage produced by hard particle impact at 1400° C appears to be more deleterious to structural integrity than that produced at 20° C under equivalent particle impact loading conditions.

1. Introduction

The properties of silicon nitride (high strength at elevated temperatures, low density, low coefficient of thermal expansion and high oxidation resistance) make it an attractive low-cost alternative to super alloys for stators, rotors and other high-temperature engine components. A major concern, however, when using silicon nitride components in flying turbines is the sensitivity of their load-bearing capacity to flaws and cracks. Aircraft turbine engines ingest solid particles during flight, and the resulting impacts can produce cracks that could reduce the strength below that necessary to sustain design loads, thereby causing catastrophic failure.

Recent research efforts [1] have established the failure phenomenology and the strength degradation effects [2] of impact-induced cracks in Si_3N_4 at room temperatures. However, similar information is lacking at the elevated temperatures representative of gas turbine service conditions. This paper describes initial results of impact experiments on Si_3N_4 at 1400° C and compares the damage observations with those from room temperature experiments.

2. Experimental procedure

Octagonal specimens roughly 25 mm in diameter were cut from a 6.35 mm thick plate of fully dense NC132 hot-pressed silicon nitride (HP Si_3N_4) purchased from the Norton Company, Worchester, Mass. The microstructure consisted of β-Si_3N_4 grains, most of which were equiaxed and less than 1 μm in size, although some were up to 4 μm long with aspect ratios up to 10. No significant grain boundary or inclusion phases were observed, but traces of tungsten carbide and tungsten disilicide were detected by X-ray diffraction.

The impact sides of the specimens were polished and the specimens were placed into a central verticle refractory tube of a furnace onto a 12 mm thick silicon nitride slab supported by an inner tube. The particle impact apparatus is shown in Fig. 1. To reduce possible effects of stress wave reflections from the rear specimen surface, the mating surfaces of specimen and slab were also ground flat and polished. The temperature of the specimens was increased to 1380 ± 20° C in about 3 h and maintained at this level for the particle impact experiments. A platinum–rhenium thermocouple monitored the temperature at the specimen location. While they were at elevated temperature, the specimens were bathed in a stream of nitrogen gas to reduce surface oxidation.

Single spheres of tungsten carbide or steel 2.4 mm in diameter were accelerated in a small gun barrel by the sudden release of compressed

*Present address: General Electric Company, Major Appliance Laboratories, Appliance Park, Louisville, Kentucky, USA.

0022–2461/81/020477–06$02.60/0

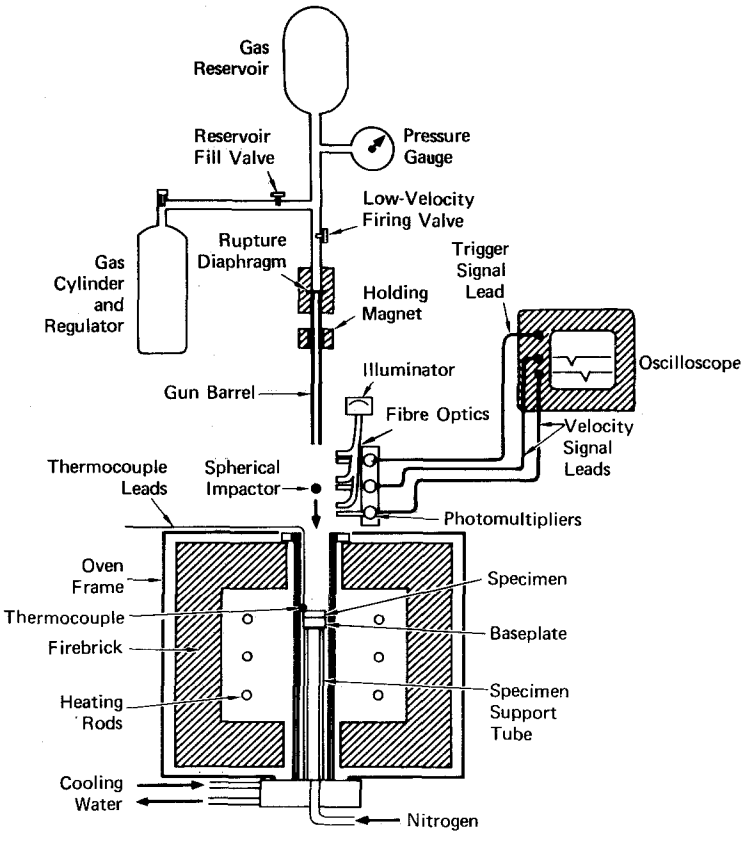

Figure 1 High temperature particle impact apparatus.

air. A thin disc located between the gas reservoir and the gun barrel sustained the compressed air until a pressure was reached which caused the disc to rupture. Rupture pressure, and hence particle velocity, was varied by using discs of different materials and thicknesses. Velocities below 85 m sec^{-1} were achieved by omitting the rupture disc, pressurizing the compressed air reservoir to a desired low pressure and opening the valve by hand. Impact velocities were measured by a photomultiplier arrangement. Light reflected by the particle into a photomultiplier at three fixed stations indicated particle position three times during its flight to the target.

3. Results

Room temperature experiments were carried out [1] at velocities ranging from 7 to 230 m sec^{-1}. No damage was produced by impacts with 2.4 mm diameter tungsten carbide spheres at velocities less than 15 m sec^{-1}. A partial ring crack appeared at 15 m sec^{-1}. Velocities between 15 and 30 m sec^{-1} produced ring cracks of increasing number and size, and velocities between 30 and 90 m sec^{-1} produced ring cracks, cone cracks and a plastic impression. Above 90 m sec^{-1}, radial cracking as well as fragmentation of the tungsten carbide sphere occurred.

Impact experiments at 1400° C were performed at velocities of 38, 51, 85, 121, 156, 173 and 197 m sec^{-1} with tungsten carbide spheres. Radial cracks and a well-defined plastic impression were produced in each experiment. The size of the impression, Fig. 2, and the intensity of the radial cracks increased with increasing velocity. At velocities greater than 150 m sec^{-1}, the radial cracks extended to the sides and rear surfaces of the specimens, often fragmenting them. Fig. 3 compares the damage at 20 and 1400° C produced by tungsten carbide spheres impacting at about 50 m sec^{-1}. The type of damage at 1400° C (radial cracks) is more deleterious than the ring-cone cracking that occurs at 20° C because radial cracks tend to be longer and deeper. Moreover, the damaged surface area is substantially larger at 1400° C. The relative dynamic hardness at 1400° C, computed from the plastic impression diameters, Fig. 2, using the Brinell equation, decreased

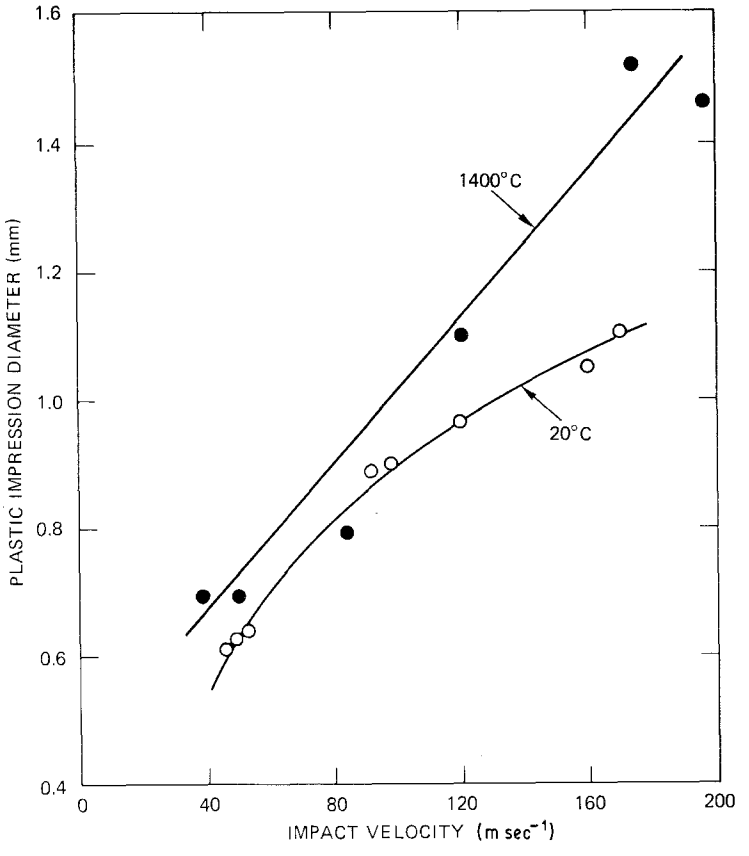

Figure 2 Plastic impression diameter against impact velocity plot for HP Si_3N_4 at room temperature and 1400° C (2.4 mm diameter WC spheres).

monotonically from 0.8 at 50 m sec^{-1} to about 0.6 at 170 m sec^{-1}.

Cone cracks occurred along with radial and lateral cracks in Si_3N_4 at 1400° C, as evidenced by the cross-section shown in Fig. 4. This fracture surface, produced by extension of radial cracks, reveals the site of the cone-shaped fragment beneath the impact site, the lateral cracks that initiate internally near the boundary of the plastic zone, the profile of the radial cracks and the microcracked zone directly beneath the plastic impression.

By contrast, the fracture damage produced by 2.4 mm diameter steel spheres consisted of annuli of segmental ring cracks both at room temperature and at 1400° C, even at velocities of 230 m sec^{-1}, [1] Fig. 5. The threshold velocity for fracture at 20° C by steel spheres was about 40 m sec^{-1}, or nearly three times as high as the threshold velocity for tungsten carbide spheres.

4. Discussion

These results show that the impact-induced fracture pattern in Si_3N_4 at 1400° C can be, but is not necessarily, different from that at 20° C. The behaviour seems to depend on the hardness of the particle relative to the target, and can be explained by a difference in the near-crater stress distribution when elastic or plastic deformation occurs in the target.

Evans, Lawn, and Wilshaw [3,4] have explained the various cracking patterns observed in ceramics around indenters and impacting particles on the basis of differences in stress states caused by the absence or the occurrence of plastic flow. When the target deforms elastically, the maximum surface tensile stresses are directed radially, resulting in an annulus of segmented ring cracks just outside the circle of contact. Higher indentation pressures or impact velocities cause these shallow ring cracks, which grow initially nearly normal to the contact surface, to extend downward and away from the zone of compression under the contact site to form cone-shaped cracks with sides roughly 50° to the impact surface or 22° to the indentation surface.

When the material under the contact area deforms plastically, radial stresses relax and the

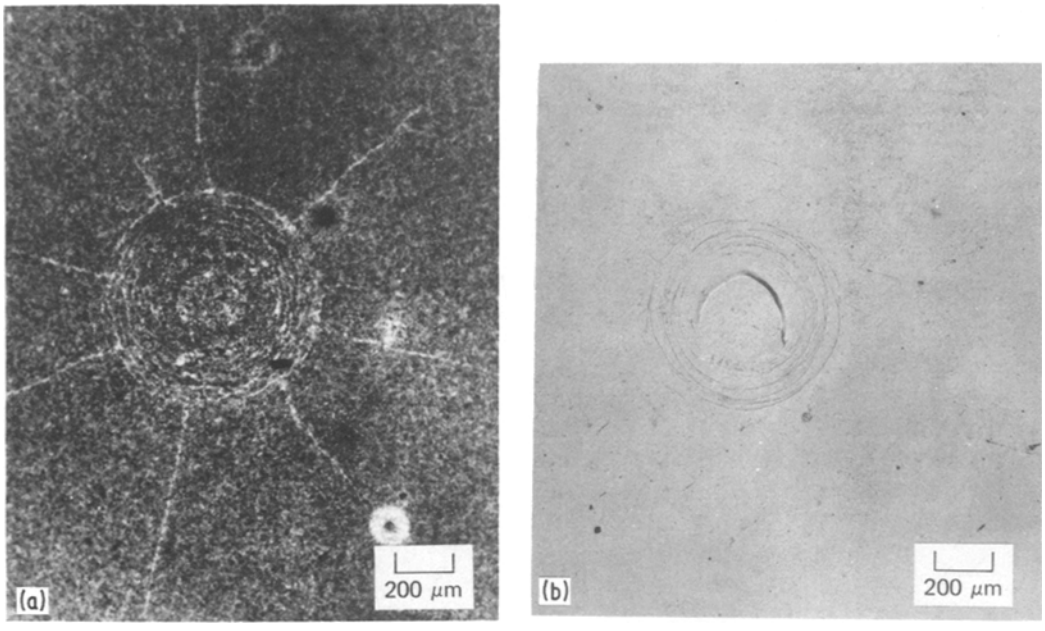

Figure 3 Surface damage in Si_3N_4 produced by 50 m sec^{-1} impact of tungsten carbide spheres at two temperatures (a) 1400° C and (b) 20° C.

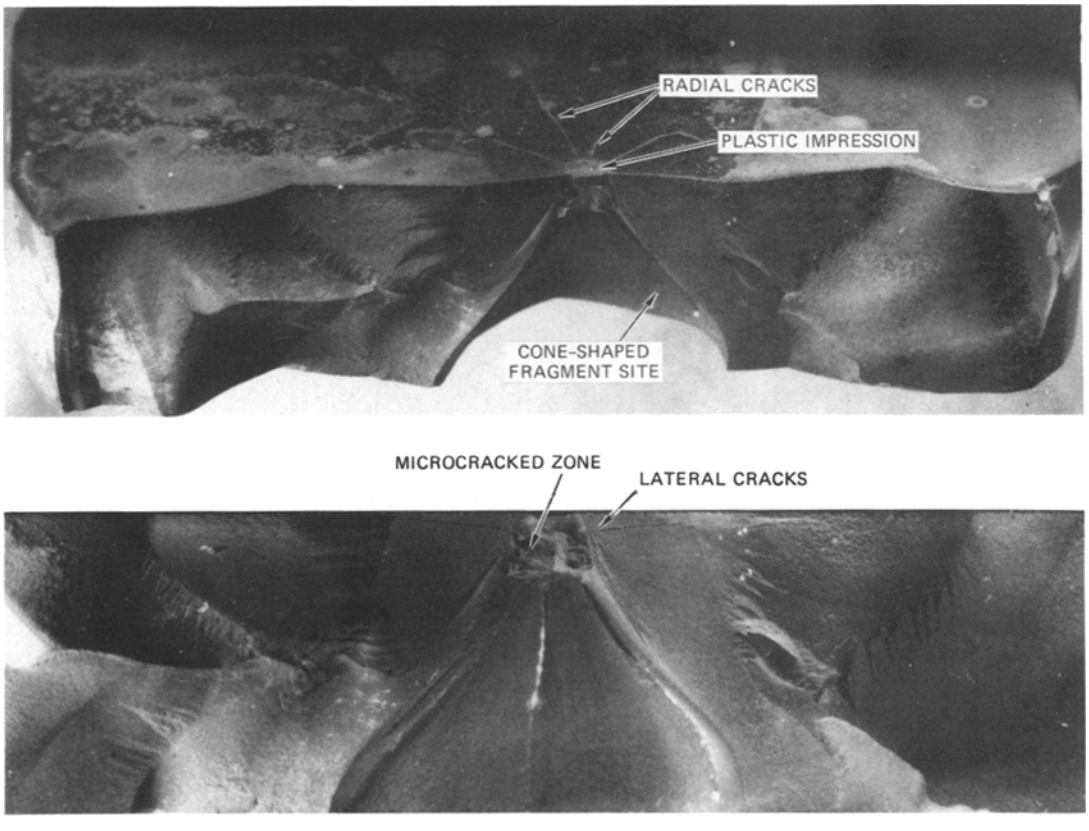

Figure 4 Side views of specimen fractured by an impacting tungsten carbide sphere.

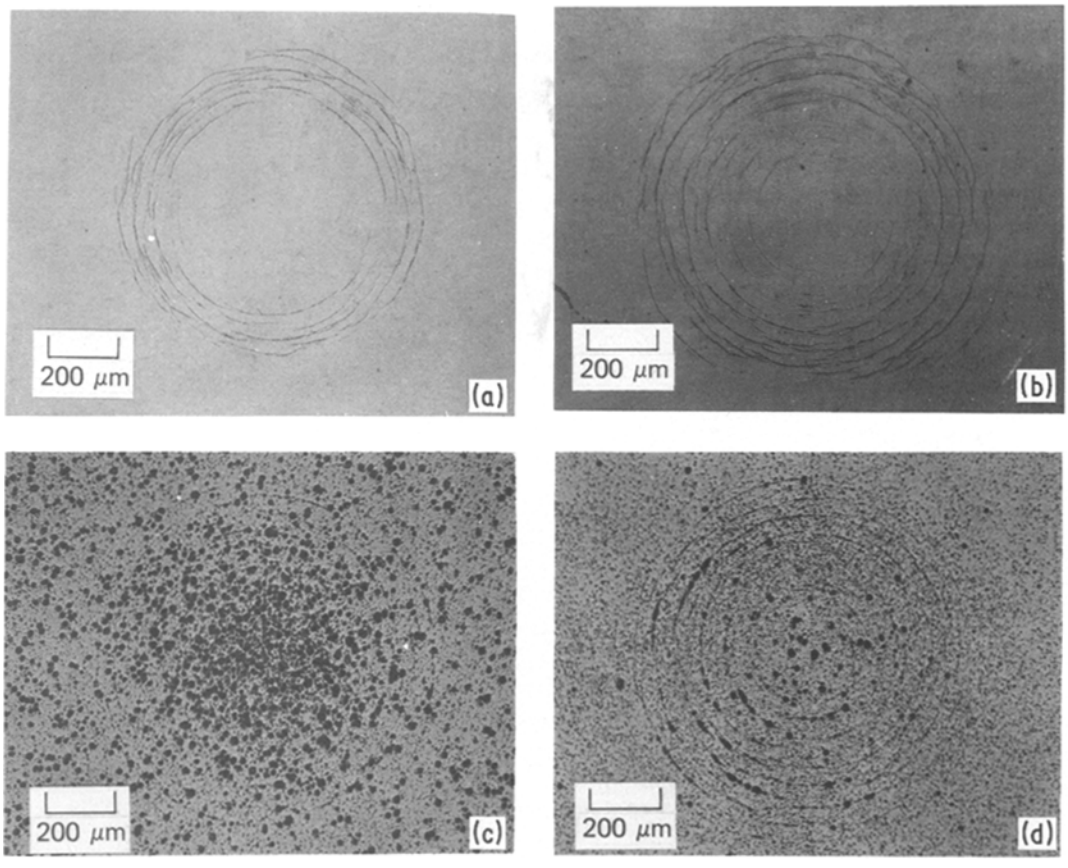

Figure 5 Surface damage in Si_3N_4 produced at two temperatures by impact of a 2.4 mm diameter steel sphere (a) 195 m sec^{-1}, (b) 231 m sec^{-1}, (c) 192 m sec^{-1} and (d) 222 m sec^{-1}. The surfaces in (c) and (d) were lightly polished to remove oxide scale.

stresses in the tangential direction become tensile, often resulting in the appearance of radial cracks extending outward from the periphery of the plastic impression in a spokelike array. Tensile stresses also arise in the specimen interior normal to the impacted surface, particularly during unloading, and may produce lateral cracks parallel to the specimen surface.

These considerations suggest that WC/Si_3N_4 impact is dominated by an elastic contact field at room temperature and by an elastic/plastic contact field at 1400° C, and therefore suggest a reversal in the relative dynamic hardness of WC and Si_3N_4 when the Si_3N_4 is heated; i.e. Si_3N_4 is harder than WC at room temperature but softer at 1400° C. Thus at 1400° C the tungsten carbide sphere remains elastic, exerts pressures equal to the Si_3N_4 hardness and the Si_3N_4 deforms. In the case of steel sphere impact, the hardness of Si_3N_4 at 1400° C must remain greater than the room-temperature hardness of the steel, so that when impact occurs, the steel deforms plastically, precluding pressures that approach the hardness of Si_3N_4 and resulting in elastic fracture.

These inferences are in agreement with relative dynamic hardness estimated from static room-temperature hardness values of 1600, 1570 and 820 kg mm^{-2} measured for the silicon nitride plates, the tungsten carbide spheres and the steel spheres, respectively. The impression diameter data in Fig. 2 show that the hardness of Si_3N_4 at 1400° C is about 80% of the room temperature hardness, or about 1300 kg mm^{-2}. Therefore, assuming similar rate effects for Si_3N_4 and WC, the WC spheres should cause elastic fracture behaviour in Si_3N_4 at room temperature, but elastic/plastic fracture behaviour at 1400° C, as was observed. Furthermore, since the hardness of the steel spheres is far below the Si_3N_4 hardness even at 1400° C, steel spheres should produce only

elastic fracture of the Si_3N_4, also as observed. The slight differences in hardness of Si_3N_4 and WC (1600 and 1570 kg mm^{-2}) will likely be enhanced in these experiments by the differences in geometry for the two materials. Geometries that constrain the plastically deformed zone more highly (such as the Si_3N_4 plate, which surrounds the plastic impression by a half space of bulk elastic material) will require higher loads for a given indentation than less constrained geometries [5] (such as the small impacting sphere).

Studman and Field [6] observed both radial and ring cracking in a quenched steel around indentations produced by tungsten carbide spheres and also explained the behaviour in terms of a transition from elastic to elastic/plastic behaviour [6].

5. Conclusions and recommendations

These results point to guidelines for predicting the type and extent of damage in Si_3N_4 turbine components to be expected from given debris particles. If indeed the relative hardnesses of particle and component govern the type of cracking in the component, a knowledge of the component hardness at the temperature of service and the hardness of the anticipated debris particles would indicate the fracture geometry and allow the propensity for strength degradation and erosion to be assessed. Cracks that tend to penetrate the component (radials, medians and cones) tend to degrade its strength, whereas cracks that tend to turn back to the surface (laterals and cones) tend to promote mass loss and erosion. A more quantitative predictive capability must await additional experiments that show the extent of damage and the resulting strength degradation and erosion behaviour as a function of relative target and particle hardnesses, particle velocity, size, shape and the number of impacts.

Acknowledgments

The authors gratefully acknowledge the financial support of the Office of Naval Research under Contract N00014-76-C-0657 and the technical direction of Dr R. C. Pohanka. Thanks are due to D. R. Curran, D. B. Marshall and D. J. Rowcliffe for reading the manuscript.

References

1. K. C. DAO, D. A. SHOCKEY, L. SEAMAN, D. R. CURRAN and D. J. ROWCLIFFE, "Particle Impact Damage in Silicon Nitride", Annual Report, Part III, to Office of Naval Research, Arlington, VA, on Contract N00014-76-C-0657, May 1979.
2. J. M. WIMMER, I. BRANSKY and N. M. TOLLAN, "Impact Resistance of Structural Ceramics, Part II Ballistic Tests", Final Technical Report, Air Force Materials Laboratory, WPAFB, Ohio, AFML-TR-76-56, December 1976.
3. B. R. LAWN and T. R. WILSHAW, *J. Mater. Sci.* **10** (1975) 1049.
4. A. G. EVANS and T. R. WILSHAW, *Acta Met.* **24** (1976) 939.
5. D. TABOR, "The Hardness of Metals" (Clarendon Press, Oxford, 1951).
6. C. J. STUDMAN and J. E. FIELD, *J. Phys. D: Appl. Phys.* **9** (1976) 857.

Received 30 April and accepted 23 July 1980.